

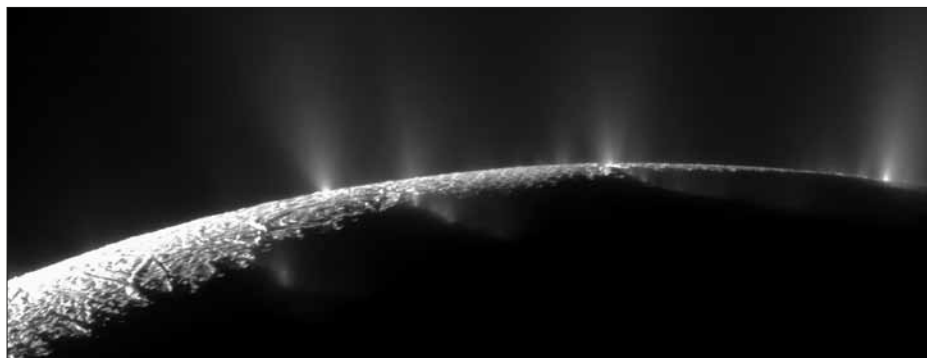
# Cassini's magnetometer at Saturn

**Michele Dougherty** and the **Cassini magnetometer team**

pick some highlights of this successful discovery mission.

Exactly one month shy of 20 years after its 15 October 1997 launch from Cape Canaveral, the Cassini-Huygens (hereafter referred to as Cassini) NASA-ESA spacecraft will end its life by burning up in the atmosphere of Saturn. This conclusion has been designed to protect any of the potentially habitable moons of Saturn (in particular Enceladus and Titan) from possible contamination by the spacecraft. It ends a mission that has been a resounding and demonstrable success: many scientific discoveries, thousands of published research papers, hundreds of graduated PhD students, and widespread excitement and inspiration among the general public and schoolchildren alike. The Cassini mission has been a truly international endeavour in which thousands of scientists and engineers from around the world, and from many different cultures, worked together towards a common goal.

The UK-led magnetometer (MAG) team, has Imperial College as the principal investigator institute, UK co-investigators based at the University of Leicester and University College London, and international co-investigators from Germany, Hungary and the United States. The instrument is a dual-sensor suite, with a fluxgate magnetometer (FGM) designed and built at Imperial College, and a vector helium/scalar sensor (V/SHM) designed and built at the Jet Propulsion Laboratory, California. These sensors are located halfway along and at the end of the spacecraft's 11 m magnetometer boom. A year after Saturn orbit insertion, which occurred on 1 July 2004, the V/SHM stopped operating, resulting in a much more complicated data calibration procedure, involving regular rolls of the entire spacecraft in a quiet background magnetic field. These rolls must be executed about two distinct axes to enable calibration of FGM data. This illustrates the collaborative approach within the Cassini team: these calibration rolls impact on the



1 Plumes of water ice and vapour erupting from locations along the "tiger stripes" near the south pole of Saturn's moon Enceladus. (NASA/JPL/Space Science Institute)

science return from other instruments, but were accepted as necessary for the MAG team to fulfil their science objectives.

To cover all of the science return from the MAG team is beyond the scope of this article. Instead, we focus on some of the highlights, including the MAG-led discovery of a water vapour plume at Enceladus;

planetary-period oscillations which fill the magnetosphere and potentially mask the signals of the internal dynamo planetary magnetic field; field-aligned currents (FACs)

and the resulting aurora. We will also highlight results related to the moon Titan and the magnetosphere of Saturn. We end the article with a description of the end-of-mission science orbits – the "Grand Finale" (figure 9) – which were designed with MAG and gravity observations in mind.

## Discovering the plume at Enceladus

On 17 February 2005, the first targeted fly-by of the moon Enceladus took place at a distance of 1265 km (the diameter of Enceladus is 500 km). Before this, ground-based observations and data from the Pioneer and Voyager spacecraft (in the late 1970s and early 1980s) had indicated that the surface of Enceladus had relatively few craters and was mainly smooth with some extensive linear cracks. The surface was dominated by water ice and seemed to have been resurfaced. It had also been postulated that Enceladus could be the source of the material in Saturn's extensive, diffuse E ring (for a summary of the history of Enceladus observations, see Dougherty

*et al.* 2017). On this first Cassini fly-by, MAG observations revealed a clear perturbation near the moon, which was interpreted as a signature of the nearly corotating Saturn plasma, and the magnetic field that was "frozen in" to this plasma, being deflected and slowed around the moon; Enceladus seemed to be acting as an unexpectedly

.....  
**"Enceladus is one of the prime potentially habitable locations in our solar system"**

large obstacle. In addition, there was an increase in ion cyclotron wave activity produced by water group ions near Enceladus, implying that the moon itself was

adding water group ions to the flowing, ambient magnetospheric plasma.

The second planned Enceladus fly-by on 8 March 2005 reached a closer altitude of 500 km. MAG data revealed very similar signatures, both the "draping" of the magnetic field around the moon and an increase in the power of water group ion cyclotron waves. This confirmed the instinct of the team that there was some atmospheric interaction – with unknown source – at Enceladus. Because the gravitational field of Enceladus is relatively small, such a source would need to be strong in order to maintain the presence of an "atmosphere" for both fly-bys. The team produced a schematic of the potential diffuse, extended atmosphere (figure 2a).

Based on the observations from these two fly-bys, the MAG team made the case to the Cassini Project that there was potentially an atmosphere of water group ions at Enceladus, which was holding off the Saturn field lines from the surface of the moon. The team requested that the third fly-by,

on 14 July 2005, approach much closer to the surface in order to investigate. This was agreed by the project team and Cassini's third fly-by reached an altitude of 173 km. This time, multiple Cassini instruments obtained definitive evidence for active ejection of water vapour and ice particles from the south pole of Enceladus.

The resulting magnetic field observations confirmed the atmospheric signature but indicated that the "atmosphere" was focused at the south pole, as revealed in figure 2b. The various instrument data sets from this third fly-by revealed a moon with internal heat leaking out of cracks at the south pole, and a water-vapour plume filled with dust and organic material rising hundreds of kilometres above the surface (figure 1, see Dougherty *et al.* 2017).

Based on this plume discovery, the Cassini extended missions were designed to further investigate Enceladus, which is now regarded as one of the prime potentially habitable locations within our solar system.

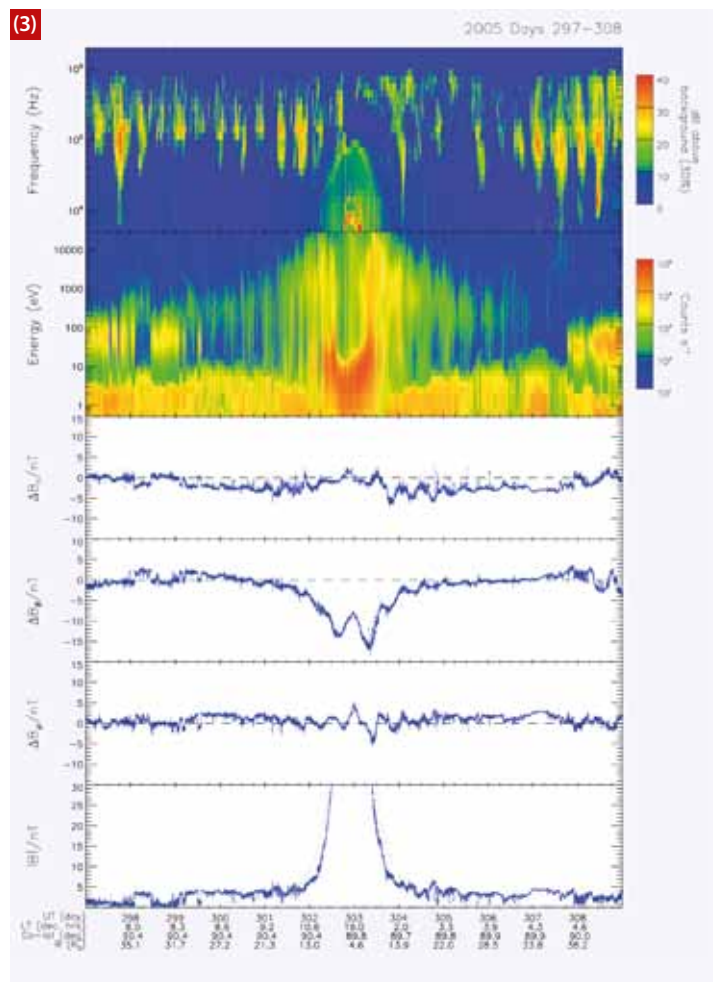
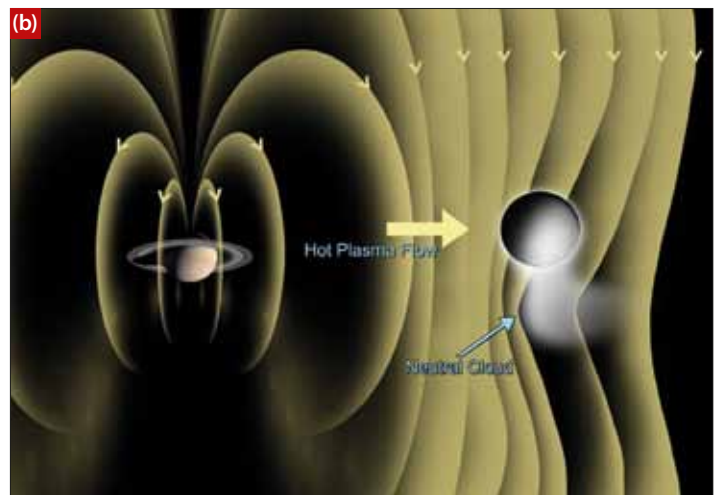
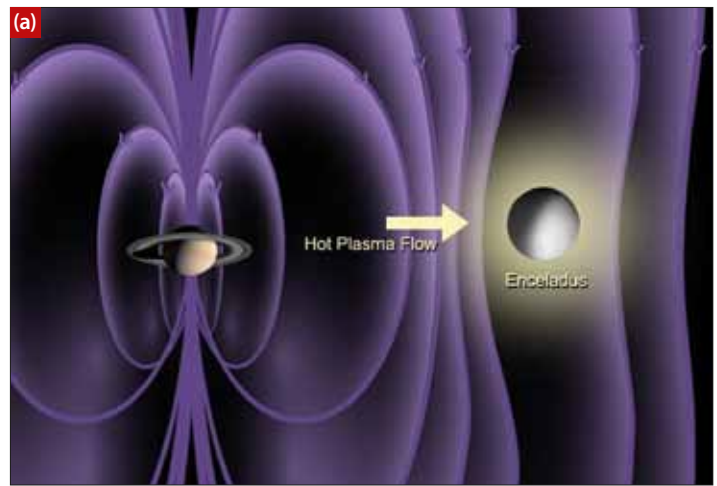
### Planetary period oscillations

The phenomenon of planetary period oscillations (PPOs) appears to be unique to Saturn's magnetosphere. In the PPOs, all the magnetospheric field and plasma parameters oscillate at near the planetary rotation period, despite the planetary magnetic field being, as far as we know, perfectly symmetrical about the planet's spin axis. The plasma parameters oscillate at the planetary rotation period in Jupiter's magnetosphere, but that is because Jupiter's magnetic dipole is tilted by  $\sim 10^\circ$  to its rotation axis, so that both the field and the embedded plasma "rock" up and down at the rotation period as the planet spins. Cassini MAG data have shown, however, that the tilt of Saturn's planetary magnetic dipole is less than  $\sim 0.1^\circ$  (Burton 2010).

The existence of PPOs at Saturn was first detected in power modulations of planetary radio emissions observed by the two Voyager spacecraft in 1980. These radio modulations were interpreted as revealing the deep rotation period of the planet via some rotating magnetic anomaly – similar, in principle, to what happens at Jupiter. The period thus determined,  $\sim 10.656$  h, remains as the IAU System III period (Desch & Kaiser 1981), in the absence of a more definitive value. Oscillations near a  $\sim 10$  h period were also observed in the energetic particle and magnetic data from the Pioneer 11 and Voyager fly-bys (Carbary & Krimigis 1982, Espinosa & Dougherty 2000), but they proved not to be consistent with a rotating magnetic anomaly within the planet (Espinosa 2003). Remote radio observations by the Ulysses spacecraft, over  $\sim 10$  years starting in 1993, showed that the radio modulation period varies slowly with time,

**2** (a) A schematic (with Saturn and Enceladus not shown to scale) showing the corotating Saturn magnetic field and plasma being draped ahead of Enceladus by a diffuse, extended atmosphere. (Dougherty *et al.* 2006) (b) Revised schematic showing the corotating Saturn magnetic field and plasma being perturbed by the polar plume of water vapour generated at the south pole of Enceladus. (Dougherty *et al.* 2006)

**3** Twelve days of Cassini magnetospheric data during Rev. 17 in 2005, with multiple magnetopause boundary crossings inbound at mid-morning on days 298 and 299, periapsis near dusk at the end of day 302, and an outbound magnetopause crossing pre-dawn on day 307. The top panel shows a radio wave power spectrogram from 5 kHz to 2 MHz, the second panel a thermal electron flux spectrogram from  $\sim 0.5$  eV to  $\sim 30$  keV, and the four lower panels show the three components and magnitude of the magnetic field. The components are spherical polar, referenced to the northern spin/magnetic axis of the planet, and have the internal field of the planet subtracted. The data at the bottom give the day number and spacecraft position – local time (hours), co-latitude and radial distance (in Saturn radii,  $R_S = 60\,268$  km). PPO-related  $\sim 10$  h modulations are evident in all parameters, and inbound magnetopause location. (Modified from Gérard *et al.* 2006)



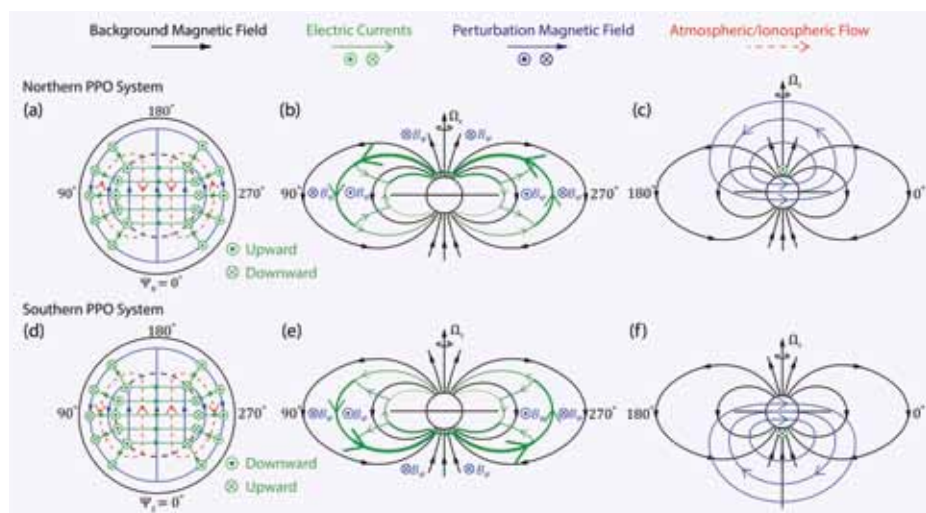


by up to  $\sim 1\%$  per (Earth) year (Galopeau & Lecacheux 2000), much too fast to be associated directly with planetary rotation.

Data acquired after Cassini's Saturn orbit insertion in 2004 showed that PPOs are ubiquitous in Saturn's magnetosphere, and are associated with modulations of the magnetic field, plasma particle properties, and waves that rotate around the planet with a  $\sim 10$  h period throughout the magnetosphere, as illustrated in figure 3. Radio observations subsequently revealed two PPO systems, simultaneously, at Saturn: one associated with the northern polar region and the other with the southern, rotating with slightly different (and drifting) periods (Gurnett *et al.* 2009). During the early Cassini mission ( $\sim 2004$ – $2007$ , post-solstice southern summer, figure 3), the southern magnetic oscillation was found to be dominant by a factor of  $\sim 3$  in amplitude, and to have a longer period ( $\sim 10.8$  h) than the northern oscillation ( $\sim 10.6$  h).

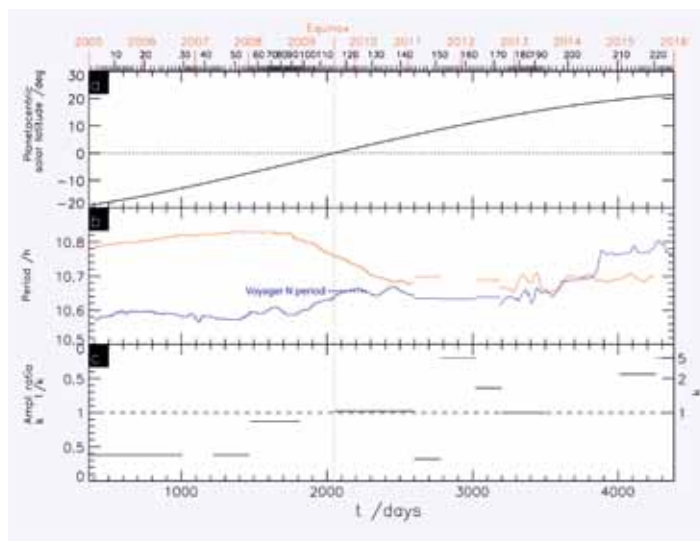
Further analyses have revealed that the PPOs are not driven from Saturn's interior, but arise from large-scale, rotating systems of electric current, which extend out from the two polar ionospheric regions, as illustrated in figure 4 (Southwood & Kivelson 2007, Andrews 2010a, 2010b, Southwood & Cowley 2014, Hunt *et al.* 2015). These currents appear to be generated by rotating twin-vortex flows in the northern and southern polar thermosphere–ionosphere regions (shown as red dashed lines on the left side of figure 4). The effect of these vortical flows, whose physical origin is uncertain, then spreads outwards along the polar field lines (arrowed black lines) into the magnetosphere, propagating in wave-like fashion through the subcorotating magnetospheric plasma (Jia *et al.* 2012, Hunt *et al.* 2014). The associated current systems are shown in the centre of figure 4, where the FACs generated in one hemisphere close partly across the field within the magnetosphere, and partly in the opposite ionosphere. The currents act to transmit force from the atmospheric flow to the magnetosphere, causing “cam-like” rotating displacements of plasma. The effects of these plasma displacements are seen in figure 3 (Burch *et al.* 2009), and give rise to PPO coupling between the northern and southern hemispheres (Hunt *et al.* 2015, Provan *et al.* 2016). Radio enhancements occur whenever the main rotating region of (upward-directed) FAC in a given hemisphere passes over the auroral emission source regions being observed – when this happens, electrons are further accelerated downward, leading to stronger emission of both radio waves (Saturn kilometric radiation or SKR, Lamy *et al.* 2010, 2013) and ultraviolet auroras (Nichols 2010a,b).

The rotating pattern of magnetic



**4** The upper and lower rows of the figure illustrate the northern and southern PPO-related current systems (green lines and symbols) and perturbation magnetic fields (blue lines and symbols), respectively. Circled dots and crosses denote vectors pointing out of and into the plane of the diagrams. The sketches on the left show views of the polar ionospheres looking down from the north, “through” the planet in the case of the southern system. The red dashed lines show the sense of the driving twin-cell flows in the thermosphere/ionosphere. Position with respect to these systems is defined by the northern and southern phases,  $\Psi_N$  and  $\Psi_S$ , as shown. The central sketches show the principal PPO-related currents in the  $\Psi_{N,S}$   $90^\circ$ – $270^\circ$  meridian planes, where the black lines show the near-axisymmetric background magnetic field. The sketches on the right show the PPO-related magnetic perturbations in the orthogonal  $\Psi_{N,S}$   $0^\circ$ – $180^\circ$  meridian planes. (Adapted from Hunt *et al.* 2015)

**5** Plot showing PPO properties over the 11 years from 2005 to 2015. Time at the bottom is given in days since the start of 2004, with year boundaries at the top, together with Cassini Rev. numbers at periapses. The top panel shows the solar latitude at Saturn, spanning nearly half a Saturn year. Vernal equinox (August 2009) is marked by the red vertical dotted line. The centre panel shows the northern (blue) and southern (red) PPO periods derived from Cassini MAG data. The blue dotted line shows the Voyager northern PPO period (see text). The bottom panel shows the north/south PPO amplitude ratio  $k$ , plotted directly for  $0 < k < 1$  (southern dominant), and as  $1/k$  in the upper half for  $1 < k < \infty$  (northern dominant). Dotted lines indicate lower limits on  $k$  for intervals when the southern PPO could not be discerned (indicating  $k > 5$ ).



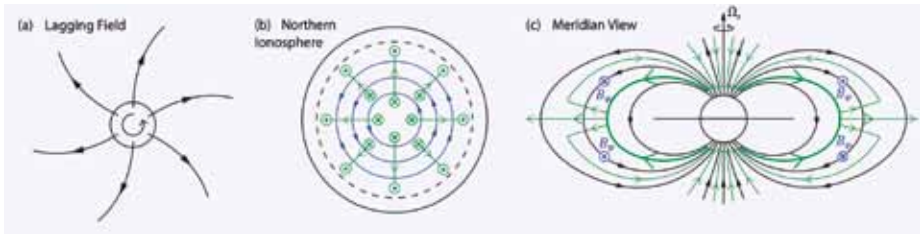
The centre panel

shows the northern (blue) and southern (red) PPO periods derived from Cassini MAG data. The blue dotted line shows the Voyager northern PPO period (see text). The bottom panel shows the north/south PPO amplitude ratio  $k$ , plotted directly for  $0 < k < 1$  (southern dominant), and as  $1/k$  in the upper half for  $1 < k < \infty$  (northern dominant). Dotted lines indicate lower limits on  $k$  for intervals when the southern PPO could not be discerned (indicating  $k > 5$ ).

perturbations produced by the rotating currents is shown by the blue lines and symbols in figure 4, both systems producing a region of quasi-uniform perturbation field in the planet's equatorial region closing over the corresponding planetary pole (Provan *et al.* 2009) (right-hand diagrams). Observed field oscillations can yield a model of the orientation of the current systems over time, and of the two rotation periods (Andrews *et al.* 2010b, 2012). Field oscillations observed over either planetary pole correspond solely to the relevant hemisphere, while oscillations observed

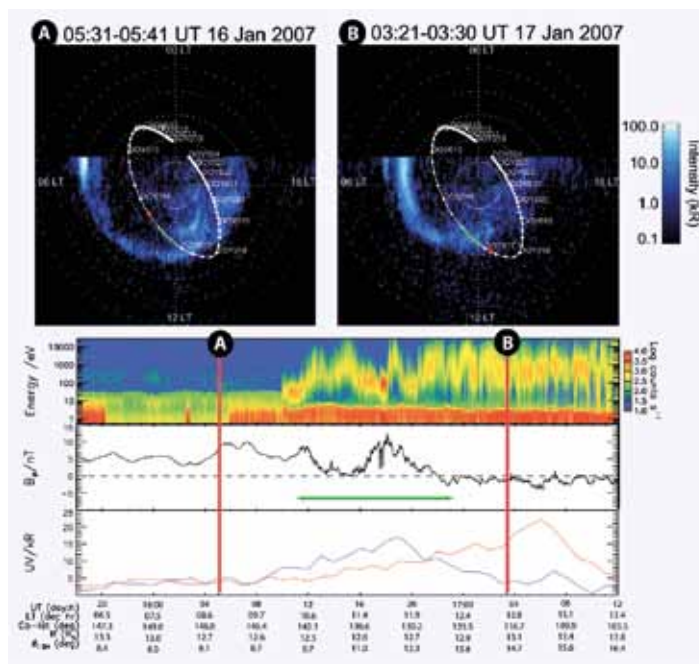
on equatorial orbits correspond to superposition of the two perturbation field patterns, leading to beat effects (with time-scale typically tens of days). The northern and southern oscillations are discernible because they produce different polarizations in the field components.

Such analyses have allowed the derivation of the rotation phase and period of the two PPO systems over essentially the whole of the Cassini mission to date (Andrews *et al.* 2012, Provan *et al.* 2013, 2016). These ephemerides also help organize other observations, such as auroral emissions



**6** Figures illustrating the magnetic field perturbations and currents associated with plasma subcorotation in Saturn's magnetosphere. (a) shows the "lagging" field that results from the magnetosphere–ionosphere coupling currents viewed looking down on Saturn's north pole. Arrowed black lines represent the magnetic field lines. (b) and (c) show the currents (green arrowed lines and symbols) and perturbation fields (blue arrowed lines and symbols) in both the northern ionosphere and in a meridian plane, respectively. Circled crosses and dots indicate vectors pointing into and out of the plane of the diagrams, respectively. The arrowed black lines indicate the near-axisymmetric background magnetospheric field. (Adapted from figure 1 of Hunt *et al.* 2014)

**7** Joint observations from two consecutive HST images (A and B) taken in January 2007. The *in situ* data panels below indicate a CAPS energy–time electron spectrogram (top panel), the azimuthal magnetic field (MAG) component in nT (middle panel), and the HST UV auroral brightness in kR (bottom panel). (From Bunce 2012)



and boundary motions (e.g. Clarke *et al.* 2010, Badman *et al.* 2012, Thomsen *et al.* 2017). Rotation periods can also be estimated from analysis of SKR modulations when separated into northern and southern components (details in e.g. Gurnett *et al.* 2009). The SKR- and MAG-derived rotation periods generally show good agreement (Provan *et al.* 2014, 2016).

PPO characteristics derived from Cassini magnetic data over the interval 2005–2015 are shown in figure 5, from just after southern solstice (October 2002) to just before northern solstice (May 2017), via vernal equinox in August 2009. Southern oscillations dominated ( $k < 1$ ) during the early part of the Cassini mission, with southern period longer than northern. Across the equinox, however, the two amplitudes became near-equal ( $k \sim 1$ ), while the two periods slowly converged towards the end of 2010, leading to the expectation of northern system dominance and period reversal as northern spring progressed. Instead, there followed a ~2.5-year interval of disturbed behaviour in which the relative

amplitudes varied strongly on ~100–200-day intervals, with fluctuating periods. The origin of this behaviour remains uncertain, with debates regarding the possible roles of the Great White Spot storm in December 2010 and new solar activity, following the recent prolonged solar cycle minimum (Provan *et al.* 2015). Following the disturbed interval, however, the periods coalesced for about ~1 year (mid-2013 to mid-2014), implying interhemispheric coupling, before separating again with the northern period enduring longer than the southern for the first time in the mission. Seasonal dependence of the PPO periods is thus indicated, possibly via varying insolation and ionospheric conductivity, although additional factors are implied by the complex post-equinox behaviour. The blue dotted line in figure 5 marks the Voyager "discovery" PPO period, observed in radio emission during approach near vernal equinox in 1980, but shifted in time by one Saturn year. This value corresponds to the northern system PPO period (right-hand polarized SKR), and agrees well with the Cassini

determination one Saturn year later, indicating some consistency with season.

### FACs and the aurora

Before the Cassini mission, Cowley *et al.* (2004a,b) modelled the main plasma flows in Saturn's magnetosphere and the associated electric current systems in the magnetically conjugate regions of Saturn's polar ionosphere. With increasing equatorial radial distance from Saturn, the first component is a region dominated by planetary rotation, where the plasma subcorotates on closed magnetic field lines, as first described for Jupiter by Hill (1979). Surrounding this region, the second component is where plasma is lost down the dusk tail via the stretching of magnetic field lines followed by plasmoid formation and pinch-off, as first described for Jupiter by Vasyliunas (1983). The third, outer region is driven by the solar wind interaction at the dayside and in the dawn tail, forming a modified Dungey cycle for Saturn (Dungey 1961). These subcorotating plasma flows produce a four-ring pattern of FACs, with distributed downward current across the polar cap, a narrow ring of upward current at the boundary between open and closed magnetic field lines, and regions of distributed downward and upward FAC on closed field lines at lower latitudes, associated with angular momentum transfer from ionosphere to magnetosphere.

Cowley *et al.* (2004a,b) proposed that the main auroral emission at Saturn is associated with the narrow ring of upward current located near the open–closed field line boundary. A simplified large-scale current system that is fundamental to this subcorotation process is shown in green in the right-hand sketch of figure 6. This current system flows down field lines (black in figure 6) into Saturn's ionosphere at higher latitudes, equatorward in the ionosphere and upward at lower latitudes, forming an axisymmetric ring around the poles in both hemispheres (shown in the centre of figure 6 for the northern hemisphere). The upward-directed currents are positioned just equatorward of the boundary between open and closed field lines, and are directly related and co-located with the remotely observed auroral and radio emissions. These FACs then close in the magnetosphere through the equatorial plasma as outward radial currents, thereby completing the circuit. The resulting azimuthal perturbation field ( $B_\phi$ ) is shown by the blue symbols. In addition, superimposed on this system are the two PPO current systems, whose currents flow at similar latitudes and with similar amplitude. The addition of the subcorotating and PPO current systems results in a combined FAC pattern which is strongly modulated according to the phase



of the PPO field perturbations (see above). Depending on these PPO phases, vastly different FAC current signatures are observed in the Cassini magnetometer data (Hunt *et al.* 2014, 2015, 2016).

Orbits in 2006 and 2007 provided the first opportunity for Cassini to directly sample the large-scale FAC current systems at Saturn associated with magnetosphere-ionosphere coupling in Saturn's dayside magnetosphere. Near-simultaneous Hubble Space Telescope (HST) observations showed Saturn's auroral oval and strong upward FAC were co-located close to the boundary between open and closed field lines (Bunce *et al.* 2008), and were in good agreement with theoretical discussions of Cowley *et al.* (2004a,b). Figure 7 summarizes these conjugate observations. The top two panels show UV images from HST of Saturn's southern auroral oval (A and B). The white tracks show the magnetically mapped footprint of Cassini. The red dots show the position of Cassini at the time of the exposure. The panels below show the *in situ* electron energy spectrogram, the azimuthal field component  $B_\phi$ , and the UV intensity from the image A (red) and image B (blue). The red vertical lines show the HST image-adjusted times. The green arrows show the region of upward FAC as identified from  $B_\phi$ , as also shown on the HST images. Bunce *et al.* (2008) showed that this upward current region was adjacent to the open field region, identified from the lack of electrons. It was also shown that these currents could account for the observed UV intensity, given the acceleration of downgoing electrons (Cowley *et al.* 2008). This interval allowed examination of the auroral region on the dayside of the planet. A second interval of high-latitude exploration in 2008 consisted of 40 passes through the auroral FACs near midnight. They revealed two clear morphological states: type 1, a mainly "lagging" azimuthal field configuration; and type 2, with a strong "leading" azimuthal field (leading relative to the ionospheric footprint of the field line) (Talboys *et al.* 2011), although the origin of these states was not then understood.

Recently, with new knowledge of the PPOs, the 2008 data set was re-examined. The FAC signatures were organized according to the phase of the rotating PPO systems, as determined by Andrews *et al.* (2012). By exploiting the anti-symmetry of the subcorotation (PPO-independent) current system shown in figure 5, and the PPO current systems shown in figure 3, the two systems were separated and shown to be comparable in amplitude and approximately co-located just equatorward of the open-closed field line boundary (Hunt *et al.* 2014, Jinks *et al.* 2014). The southern hemisphere FAC morphology, strength

and position were shown to be strongly modulated by the southern PPO phase. The northern hemisphere data set for this time interval was more complex. Here, the FAC morphology and strength were modulated not only by the northern PPO system, but also by the southern PPO system (Hunt *et al.* 2015). This gave the first direct evidence for the interhemispheric closure of the southern PPO system into the northern ionosphere (Southwood & Kivelson 2007, 2009). There is a direct link between regions of upward FAC and downgoing electrons and PPO modulations have been observed in Saturn's infrared and ultraviolet auroral intensity, power and location (Nichols *et al.* 2008, 2010a,b, Badman *et al.* 2012, Bunce *et al.* 2014).

During the high-latitude passes, we have also seen unusual FAC events associated with solar-wind-driven global magnetospheric dynamics. For example, during revolution 89 in 2008, an extraordinarily strong upward-directed FAC signature was observed, accompanied by hot plasma signatures at very high latitude in the polar cap. It was suggested that this event was due to an episode of rapid tail reconnection, triggered by a sudden solar-wind shock compression of the magnetosphere (Cowley *et al.* 2005, Bunce *et al.* 2010). A further example was seen in 2013, additionally revealing unusual auroral morphology (Badman *et al.* 2016).

### Saturn's magnetosphere

Saturn's magnetosphere is one of the largest in the solar system. Cassini magnetic field observations have allowed characterization of the highly variable solar wind at Saturn orbit (e.g. Jackman & Arridge 2011a). The typical solar magnetic field at Saturn is consistent with the "Parker spiral" prediction (Jackman *et al.* 2008a), and the solar wind generally comprises alternating regions of compression and rarefaction (Jackman *et al.* 2004). The shock wave in the solar wind in front of the magnetosphere and the downstream magnetosheath region have also been investigated (Bertucci *et al.* 2007, Achilleos *et al.* 2006, Went *et al.* 2011a, Masters *et al.* 2011, 2013, Sulaiman *et al.* 2014, 2015, 2016), confirming that the shock has one of the highest Mach numbers in the solar system. Much work has focused on spacecraft crossings of the magnetopause boundary of Saturn's magnetosphere, revealing mass and energy transport processes (Masters *et al.* 2009, 2010, 2012, Cutler *et al.* 2011, Lai *et al.* 2012, Badman *et al.* 2013).

Thanks to Cassini, the typical internal configuration of Saturn's magnetosphere is now well understood. The magnetopause

location is controlled by total pressure balance, and is typically ~25 Saturn radii ( $R_S$ ) sunward of the planet along the Saturn-Sun line (Arridge *et al.* 2006, Achilleos *et al.* 2008, Pilkington *et al.* 2014, 2015a). Saturn has no clear "cushion region" in the outermost magnetosphere, as observed at Jupiter (Went *et al.* 2011b); however, a similarity with Jupiter's magnetosphere lies in the radial distension of the planetary magnetic field lines to form a "magnetodisc" (Arridge *et al.* 2007, 2008a, Bunce *et al.* 2007, Achilleos *et al.* 2010a,b). This arises from the appreciable amount of magnetospheric plasma that is forced to rotate with the planetary magnetic field, one result of which is a radially outward centrifugal force that contributes to an equilibrium magnetodisc field structure.

Saturn's obliquity and near-aligned rotation and magnetic dipole axes produce a seasonal effect where the outer dayside

..... magnetodisc is pushed northward, because of the proximity of the subsolar magnetopause, under southern summer conditions (and probably vice versa) (Arridge

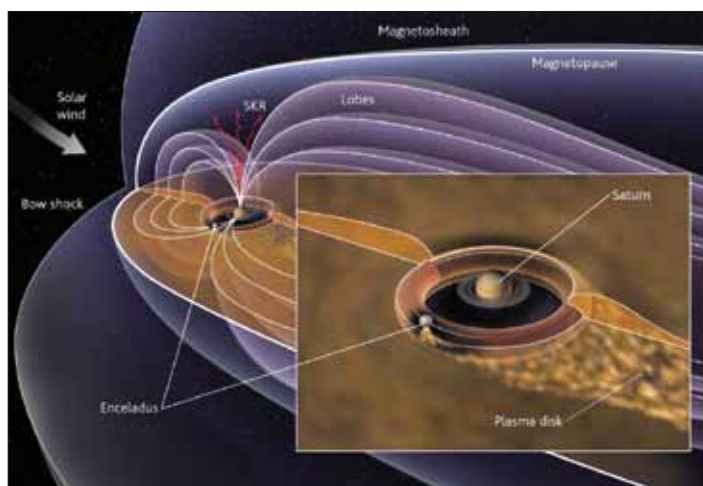
**"The influence of Saturn's intrinsic magnetic field extends far out into space"**

*et al.* 2008b). On the nightside, the magnetic field lines of the outer magnetosphere extend to form a long magnetotail (Arridge *et al.* 2008b, Jackman & Arridge 2011b). The structure of Saturn's inner magnetosphere shows less deviation from the pure planetary field. However, the magnetometer discovery of the moon Enceladus as a strong plasma source explains much of the configuration of Saturn's global magnetosphere as a consequence of significant internal plasma mass loading (Dougherty *et al.* 2006, Kivelson 2006), as shown in figure 8.

Cassini magnetic field observations have also shown how dynamic Saturn's magnetosphere is. The solar wind dramatically compresses and expands the system (Arridge *et al.* 2006, Achilleos *et al.* 2008), capable of producing an auroral response (Badman *et al.* 2005, 2008), and with additional control of the magnetopause position related to the internal state of the magnetosphere (Pilkington *et al.* 2015b, Sorba *et al.* 2017) and to the influence of the PPOs. Magnetic reconnection at the magnetopause drives a cycle equivalent to the terrestrial Dungey cycle (Cowley *et al.* 2004a, Jackman *et al.* 2005, Badman *et al.* 2005, Masters *et al.* 2014, Masters 2015). Even the dayside magnetodisc is sensitive to the solar wind, since compression of the magnetopause toward the planet can effectively "dipolarize" the field (Leisner *et al.* 2007, Arridge *et al.* 2008a).

Magnetic signatures of FACs have revealed how the magnetosphere and planetary upper atmosphere (ionosphere) are coupled, central to a global understanding of the physics of the system (Bunce *et*

**8** Schematic of Saturn's magnetosphere. (Taken from Kivelson 2006)



*al.* 2008, Talboys *et al.* 2009a,b, Badman *et al.* 2012, Hunt *et al.* 2015, 2016). Recently, periodic magnetic field variability, not directly related to planetary rotation nor to PPOs, has been reported (Yates *et al.* 2016), and is a first step in exploring Saturn's magnetospheric pulsations. Magnetic signatures of explosive energy release within the magnetotail from magnetic reconnection and related plasma transport have been widely reported and investigated, including their relationship to auroral emissions (Bunce *et al.* 2005, Jackman *et al.* 2007, 2008b, 2010, 2011, 2014, 2015, Lai *et al.* 2016, Smith *et al.* 2016). Remaining open issues concerning Saturn's magnetosphere include the mass budget of the system, and how internal and external driving of the system combine to produce the magnetospheric dynamics revealed by Cassini.

### Titan and its environment

Saturn's largest moon, Titan, is unusual, with a dense smoggy atmosphere and hydrocarbon lakes described in this issue by Coates (p4.20) and Zarnecki (p4.31). Titan's orbit at  $\sim 20$  Saturn radii places it, most of the time, within Saturn's magnetosphere, immersed in rapidly rotating, magnetized plasma that moves past the moon at  $\sim 100 \text{ km s}^{-1}$ , far faster than Titan's orbital speed of  $\sim 6 \text{ km s}^{-1}$ . As the plasma flows past and around Titan, the magnetic lines that are "frozen" to the flowing plasma drape around the moon, forming downstream lobes of strongly azimuthal field generally pointing towards Titan in one lobe, and away in the other.

The magnetic field configuration associated with this Titan–Saturn interaction depends on the conditions in Saturn's rotating magnetospheric plasma upstream of Titan. Before Cassini, the common perception was that the upstream field orientation would be north–south, the equatorial direction of Saturn's dipole field. Cassini has shown a different picture. The magnetospheric, disc-like plasma sheet continually flaps up and down past Titan with a period

close to what we believe is the true rotation period of the planet – around 10.7 hours. This flapping does not come from any tilt in Saturn's magnetic equator (Saturn's internal field is almost perfectly aligned with the planet's rotational axis). Rather, it arises from a rotating wave-like pattern imposed on the sheet by rotating systems of current in the magnetosphere, flowing on field lines extending to  $\sim 10$ – $15$  Saturn radii. As the plasma sheet moves, the upstream field changes, being dominantly north–south when Titan is near the centre of the plasma sheet, and dominantly radial (towards or away from Saturn) when Titan is just outside the sheet. These changes were characterized by Bertucci *et al.* (2009), who surveyed Cassini magnetometer data during spacecraft fly-bys of Titan. Later, Achilleos *et al.* (2014) used a model of the plasmasheet (magnetodisc) to study one fly-by in detail. They found that the magnetospheric flux tubes that flow closest to Titan may carry with them the imprint of a very different kind of upstream field compared to the imprint carried by plasma in the far-Titan space. This is because the upstream field is continually changing. This "change in magnetic imprint" could become more pronounced if the boundary of Saturn's magnetosphere moves inward or outward past Titan. When this happens (albeit relatively rarely), Titan transitions between a magnetospheric and a magnetosheath/solar-wind regime, a process first discovered by Bertucci *et al.* (2008) in the T32 Titan fly-by of Cassini.

Bertucci *et al.* (2008) noted three phases. Before the Titan encounter, Cassini observed a magnetic field (and plasma parameters) consistent with a 10-hour excursion into the magnetosheath region of Saturn, i.e. shocked solar wind plasma. Cassini was inside Titan's orbit during this interval, so it follows that Titan was immersed in magnetosheath plasma for at least 10 hours. Then the spacecraft encountered magnetospheric plasma for approximately three hours as the magnetopause

boundary moved out over Cassini; Titan too had been in the magnetosphere, for at most three hours. After another  $\sim 15$  minutes in the magnetosheath (the magnetopause having now moved back inwards past the spacecraft), Cassini reached its closest approach (CA) to Titan, which had again been exposed to magnetosheath plasma, for at least  $\sim 15$  minutes.

At CA, the magnetic field, remarkably, had a negative  $Z$  component (i. e. pointing southward). By contrast, the ambient magnetosheath field surrounding the CA interval had positive  $B_z$ . The "negative  $B_z$ " near CA is consistent with the draped field that would have been seen had Titan been continually immersed in Saturn's magnetosphere. But at CA, both Titan and Cassini were in the magnetosheath. Titan had been there for at least 15 minutes after spending up to three hours in the magnetosphere. Hence, the field that was imprinted on Titan's ionosphere during its magnetospheric excursion survived there for at least  $\sim 15$  minutes. If we assume that the long (10 hour) magnetosheath excursion well before CA completely removed any imprint of Saturn's magnetospheric field from Titan, then the later magnetospheric imprint must have then replaced this pure magnetosheath imprint during the subsequent  $\sim 3$  hours that the moon spent in the magnetosphere. Hence, this time range ( $\sim 15$  minutes –  $\sim 3$  hours) constrains the imprint or fossil field lifetime at Titan, raising the intriguing prospect of a "magnetic archaeology" where close fly-bys of Titan could potentially reveal details of ambient fields to which Titan has been exposed up to about three hours in the past.

### The beginning of the end

After 13 years in orbit around Saturn, the Cassini mission has entered its final phase. The first stage of the Grand Finale involved a ring-grazing orbital phase in which the periapse distance was just outside of the edge of the visible rings, enabling a focus on ring science as well as measurement of the FACs and the PPOs. Analysis of data from this phase is critical to the success of the Grand Finale MAG science, because an understanding of both FAC and PPO behavior is vital in order to resolve the magnetic signatures from Saturn's interior.

The 22 Grand Finale orbits, with periapse distance inside the rings, began on 28 April 2017, each lasting 6.4 days. These orbits took three years of planning in order to ensure the best possible science return from all the instruments, complicated by the fact that neither the spacecraft nor the instruments were designed to carry out such manoeuvres. MAG is prime on two of the 22 orbits in which the spacecraft is rolling around periapse, in order to enable us to calibrate

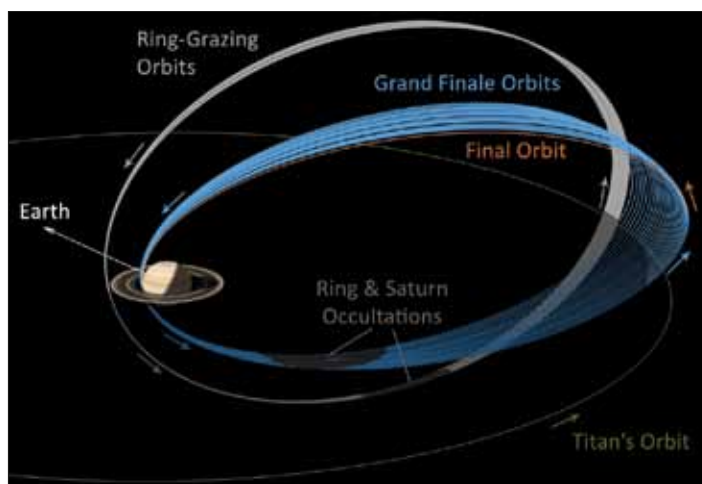


the instrument (around closest approach we are in a measuring range not active since Earth swingby in 1999). On two more orbits, we are riding along with the gravity experiment (Radio Sub System) and rolling around the z-axis of the spacecraft, again for calibration.

Cassini MAG measurements to date have greatly enhanced our understanding of Saturn's intrinsic magnetic field, but have raised many new questions as well. Saturn's intrinsic magnetic field has always been regarded as somewhat anomalous since the very first measurements made by the Pioneer 11 magnetometer (Smith *et al.* 1980). The first surprise concerned the relative weakness of the field: Saturn's surface magnetic field is only  $\sim 20000$  nT near the equator, which is  $\sim 20$  times weaker than Jupiter's surface magnetic field, and even weaker than Earth's surface magnetic field. This apparent weakness of the field is particularly surprising, given that Saturn's emitted power is the second highest in our solar system after Jupiter.

The second surprising feature is the close alignment of Saturn's magnetic axis with its spin axis. Pioneer 11 measurements were able to place an upper limit on a dipole tilt of  $1^\circ$ , to describe the possible departure from axisymmetry (Smith *et al.* 1980). Such a close alignment seems to be in contradiction to Cowling's well-known anti-dynamo theorem, which states that a purely axisymmetric magnetic field cannot be self-sustained. Only Saturn orbit insertion data have revealed any departure from an

9 Schematic of the end of mission phase with the F ring phase in white, the grand finale phase in blue and the final impacting orbit in orange.



axisymmetric offset dipole, although the spacecraft did not spend long enough close enough to the planet to reveal any longitudinal structure of that asymmetry.

The primary MAG objective of the Grand Finale orbits (figure 9) is to determine any asymmetric component of the intrinsic planetary field. With an accurate determination, Saturn's rotation rate could finally be

inferred directly. This is of great importance for construction of accurate interior models. It also sets the reference state against which the differential rotation of the atmosphere and its latitudinal dependence is defined, important for understanding the angular momentum budget of the atmospheric circulation. Continuous monitoring of the external magnetospheric field and accurate tracking of the PPOs is required in order to determine and

understand the intrinsic planetary field in its proper context.

The Cassini end-of-mission orbits will enable paradigm-shifting discoveries about Saturn's intrinsic magnetic field and interior due to the close proximity to Saturn, as well as their highly inclined nature. With high-quality MAG measurements along Cassini proximal orbits, we will be able to address several key questions concerning Saturn's interior: the rotation rate of Saturn at depth, the degree of asymmetry of the intrinsic field, and the depth to the dynamo region. With accurate field models based on measurements made during the proximal orbits, we will be able to compare characteristics of the large-scale structure of Saturn's field with other planetary dynamos and dynamo simulations. This improved knowledge will greatly enhance our understanding of the present state of Saturn's interior, as well as its formation and evolution. ●

## AUTHORS

The Cassini magnetometer team are: Michele K Dougherty, Blackett Lab, Physics Dept, Imperial College London; Nicholas Achilleos, Physics and Astronomy, University College London; Emma Bunce, Physics Dept, University of Leicester; Stanley Cowley, Leicester; Gregory Hunt, ICL; Adam Masters, ICL; and Gabby Provan, Leicester.

## REFERENCES

- Achilleos N *et al.* 2006 *J. Geophys. Res.* **111** A03201  
 Achilleos N *et al.* 2008 *J. Geophys. Res.* **113** A11209  
 Achilleos N *et al.* 2010a *Mon. Not. R. Astron. Soc.* **401A** 2349  
 Achilleos N *et al.* 2010b *Geophys. Res. Lett.* **37** L20201  
 Achilleos N *et al.* 2014 *Geophys. Res. Lett.* **41** 8730  
 Arridge CS *et al.* 2006 *J. Geophys. Res.* **111** A11227  
 Arridge CS *et al.* 2007 *Geophys. Res. Lett.* **34** L09108  
 Arridge CS *et al.* 2008a *J. Geophys. Res.* **113** A04214  
 Arridge CS *et al.* 2008b *J. Geophys. Res.* **113** A08217  
 Andrews DJ *et al.* 2010a *J. Geophys. Res.* **113** A04212  
 Andrews DJ *et al.* 2010b *J. Geophys. Res.* **115** A12252  
 Andrews DJ *et al.* 2012 *J. Geophys. Res.* **117** A04224  
 Badman SV *et al.* 2005 *J. Geophys. Res.* **110** A11216  
 Badman SV *et al.* 2008 *Ann. Geophys.* **26** 12 3641  
 Badman SV *et al.* 2012 *J. Geophys. Res.* **117** A09228  
 Badman SV *et al.* 2013 *Geophys. Res. Lett.* **40** 1027  
 Badman SV *et al.* 2016 *Icarus* **263** 83  
 Bertucci C *et al.* 2007 *J. Geophys. Res.* **112** A09219  
 Bertucci C *et al.* 2008 *Science* **321** 1475  
 Bertucci C *et al.* 2009 *Planet. Space Sci.* **57** 1813  
 Bunce EJ 2012 *Geophys. Monograph Series* **195** 397  
 Bunce EJ *et al.* 2005 *Geophys. Res. Lett.* **32** L20504  
 Bunce EJ *et al.* 2006 *Adv. Space Res.* **38** 806  
 Bunce E *et al.* 2007 *J. Geophys. Res.* **112** A10202  
 Bunce EJ *et al.* 2008 *J. Geophys. Res.* **113** A09209  
 Bunce EJ *et al.* 2010 *J. Geophys. Res.* **115** A20238  
 Bunce EJ *et al.* 2014 *J. Geophys. Res.* **119** 3528  
 Burch JL *et al.* 2009 *Geophys. Res. Lett.* **37** L14203  
 Burton ME *et al.* 2010 *Geophys. Res. Lett.* **37** L24105  
 Carbary JF & Krimigis SM 1982 *Geophys. Res. Lett.* **9** 1073  
 Clarke KE *et al.* 2010 *J. Geophys. Res.* **115** A08209  
 Cowley SWH *et al.* 2004a *Ann. Geophys.* **22** 1379  
 Cowley SWH *et al.* 2004b *J. Geophys. Res.* **109** A05212  
 Cowley SWH *et al.* 2005 *J. Geophys. Res.* **110** A02201  
 Cowley SWH *et al.* 2008 *Ann. Geophys.* **26** 2613  
 Cutler JC *et al.* 2011 *J. Geophys. Res.* **116** A10220  
 Desch MD & Kaiser ML 1981 *Geophys. Res. Lett.* **8** 253  
 Dougherty MK *et al.* 2006 *Science* **311** 1406  
 Dougherty MK *et al.* 2017 *Enceladus and the icy Moons of Saturn* in press (University of Arizona)  
 Duney JW 1961 *Phys. Rev. Lett.* **6** 47  
 Espinosa SA & Dougherty MK 2000 *Geophys. Res. Lett.* **27** 2785  
 Espinosa SA *et al.* 2003 *J. Geophys. Res.* **108** A21085  
 Galopeau PHM & Lecacheux A 2000 *J. Geophys. Res.* **105** 13089  
 Gérard J-C *et al.* 2006 *J. Geophys. Res.* **111** A12210  
 Gurnett DA *et al.* 2009 *Geophys. Res. Lett.* **36** L16102  
 Hill TW 1979 *J. Geophys. Res.* **84** 6554  
 Hunt GJ *et al.* 2014 *J. Geophys. Res.* **119** 9847  
 Hunt GJ *et al.* 2015 *J. Geophys. Res.* **120** 7552  
 Hunt GJ *et al.* 2016 *J. Geophys. Res.* **121** 7785  
 Jackman CM & Arridge CS 2011a *Sol. Phys.* **274** 481  
 Jackman CM & Arridge CS 2011b *J. Geophys. Res.* **116** A05224  
 Jackman CM *et al.* 2004 *J. Geophys. Res.* **109** A11203  
 Jackman CM *et al.* 2005 *J. Geophys. Res.* **110** A10212  
 Jackman CM *et al.* 2007 *Geophys. Res. Lett.* **34** L11203  
 Jackman CM *et al.* 2008a *J. Geophys. Res.* **113** A08114  
 Jackman CM *et al.* 2008b *J. Geophys. Res.* **113** A11213  
 Jackman CM *et al.* 2010 *J. Geophys. Res.* **115** A10240  
 Jackman CM *et al.* 2011 *J. Geophys. Res.* **116** A10212  
 Jackman CM *et al.* 2014 *J. Geophys. Res. Space Physics* **119**  
 Jackman CM *et al.* 2015 *J. Geophys. Res. Space Physics* **120** 3603  
 Jia X *et al.* 2012 *J. Geophys. Res.* **117** A04215  
 Jinks SL *et al.* 2014 *J. Geophys. Res.* **119** 8161  
 Kivelson MG 2006 *Science* **311** 1391  
 Lai H *et al.* 2012 *J. Geophys. Res.* **117** A05222  
 Lai HR *et al.* 2016 *J. Geophys. Res. Space Physics* **121** 3050  
 Lamy L *et al.* 2010 *Geophys. Res. Lett.* **37** L12104  
 Lamy L *et al.* 2013 *J. Geophys. Res.* **118** 4817  
 Leisner JS *et al.* 2007 *Geophys. Res. Lett.* **34** L12103  
 Masters A *et al.* 2009 *Planet. Space Sci.* **57** 1769  
 Masters A *et al.* 2010 *J. Geophys. Res.* **115** A02725  
 Masters A *et al.* 2011 *J. Geophys. Res.* **116** A10107  
 Masters A *et al.* 2012 *Geophys. Res. Lett.* **39** L08103  
 Masters A *et al.* 2013 *Nat. Phys.* **9** 164  
 Masters A *et al.* 2014 *Geophys. Res. Lett.* **41** 1862  
 Masters A *et al.* 2015 *Geophys. Res. Lett.* **42** 2577  
 Nichols JD *et al.* 2008 *J. Geophys. Res.* **113** A11205  
 Nichols JD *et al.* 2010a *Geophys. Res. Lett.* **37** L15102  
 Nichols JD *et al.* 2010b *Geophys. Res. Lett.* **37** L24102  
 Pilkington NM *et al.* 2014 *J. Geophys. Res. Space Physics* **119** 2858  
 Pilkington NM *et al.* 2015a *J. Geophys. Res. Space Physics* **120** 7289  
 Pilkington NM *et al.* 2015b *Geophys. Res. Lett.* **42** 6890  
 Provan G *et al.* 2009 *J. Geophys. Res.* **114** A02225  
 Provan G *et al.* 2013 *J. Geophys. Res.* **118** 3243  
 Provan G *et al.* 2014 *J. Geophys. Res.* **119** 7380  
 Provan G *et al.* 2015 *J. Geophys. Res.* **120** 9524  
 Provan G *et al.* 2016 *J. Geophys. Res.* **121** 9829  
 Smith E *et al.* 1980 *Science* **207** 407  
 Smith AW *et al.* 2016 *J. Geophys. Res. Space Physics* **121** 2984  
 Sorba A *et al.* 2017 *J. Geophys. Res. Space Physics* **122** 1572  
 Southwood DJ & Cowley SWH 2014 *J. Geophys. Res.* **119** 1563  
 Southwood DJ & Kivelson MG 2007 *J. Geophys. Res.* **112** A12222  
 Southwood DJ & Kivelson MG 2009 *J. Geophys. Res.* **114** A09201  
 Sulaiman AH *et al.* 2014 *J. Geophys. Res. Space Physics* **119** 5651  
 Sulaiman AH *et al.* 2015 *Phys. Rev. Lett.* **115** 12  
 Sulaiman AH *et al.* 2016 *J. Geophys. Res. Space Physics* **121** 4425  
 Talboys DL *et al.* 2009a *J. Geophys. Res.* **114** A06220  
 Talboys DL *et al.* 2009b *Geophys. Res. Lett.* **36** L19107  
 Talboys DL *et al.* 2011 *J. Geophys. Res.* **116** A04213  
 Thomson MF *et al.* 2017 *J. Geophys. Res.* **122** 280  
 Vasyliunas VM 1983 *Physics of the Jovian Magnetosphere* (CUP, Cambridge and New York) 395  
 Went DR *et al.* 2011a *J. Geophys. Res.* **116** A07202  
 Went DR *et al.* 2011b *J. Geophys. Res.* **116** A04224  
 Yates JN *et al.* 2016 *Geophys. Res. Lett.* **43** 11102